

Geodesy: Self-rising 2.5D Tiles by Printing along 2D Geodesic Closed Path

ABSTRACT

Thermoplastic and Fused Deposition Modeling (FDM) based 4D printing are rapidly expanding to allow for space- and material-saving 2D printed sheets morphing into 3D shapes when heated. However, to our knowledge, all the known examples are either origami-based models with obvious folding hinges, or beam-based models with holes on the morphing surfaces. Morphing continuous double-curvature surfaces remains a challenge, both in terms of a tailored toolpath-planning strategy and a computational model that simulates it. Additionally, neither approach takes surface texture as a design parameter in its computational pipeline.

To extend the design space of FDM-based 4D printing, in Geodesy, we focus on the morphing of continuous double-curvature surfaces or surface textures. We suggest a unique tool path - printing thermoplastics along 2D closed geodesic paths to form a surface with one raised continuous double-curvature tiles when exposed to heat. The design space is further extended to more complex geometries composed of a network of rising tiles (i.e., surface textures). Both design components and the computational pipeline are explained in the paper, followed by several printed geometric examples.

INTRODUCTION

From turtle shells to igloos, textured double curvature surfaces widely exist in nature and architecture. Within the context of Geodesy, we geometrically interpret these textured surfaces as a group of raised tiles from a flat or curved continuous surface. These geometries provide many use cases and rich aesthetic qualities. However, these geometries also give rise to several challenges for manufacturing. Printing these surfaces often requires numerous support structures, therefore consuming more printing time and material, increasing the risk of failure, and taking up larger space if shipped. Additionally, Smooth textures with fine resolutions are difficult and slow to print. Beyond printing, raised surfaces are often fabricated by vacuum forming or injection molding, time-consuming and high-cost processes that require molds frequently produced by CNC or Wire EDM machines.

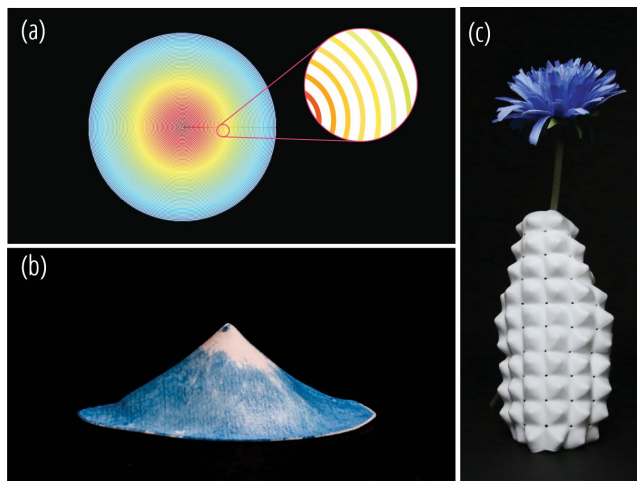


Figure 1. (a) 2D printing path for Fuji Mountain, with color showing the shrinkage rate. (b) Side view of a transformed Fuji Mountain. Color was added via screen printing before the morphing. (c) Textured vase transformed from a flat sheet.

4D printing has been devised as a way to speed up the 3D printing and prototyping process through self-folding [22]. However, existing methods of 4D printing have limited geometric design options. The output geometries are limited to 1D linear frames [7], developable surfaces [1], or non-developable surfaces with holes [23]. *To our knowledge, continuous double-curvature surfaces or surface textures have not been previously achieved via thermoplastic-based 4D printing.* Thus, Geodesy is trying to push one step further towards the goal of morphing continuous double-curvature surfaces via 4D printing. As demonstrated in the later Application section, a variety of such geometries and surface textures can be achieved with Geodesy. Fig. 1a shows a flat printing tool path that enable a flat disk to morph into a Fuji mountain (Fig. 1b). Alternatively, a group of flat tiles can form morphing textures (Fig. 1c).

In Geodesy, we introduce a novel path planning approach by printing geodesic closed curves along the outline of a tile to form a sheet. Further, we can print a group of raised tiles to form a textured surface with a desired overall geometry. The transformation of the tiles leads to their own geometries, but also contributes to the overall shape.

Additionally, we implemented a design tool which is both a simulator and a compiler. The simulator visualizes the

approximated 3D geometry after morphing and further assists the user in making informed modifications.

The main contributions are the following:

1. A novel tool path planning approach that enables the morphing of a flat tile into a continuous double-curvature surface, or a group of flat tiles into surface textures.
2. A simulation tool that visualizes the morphing via a tailored mass-spring model and compiles the design input (2D patterns of tiles) into G-code for 3D printing.
3. Geometric design components corresponding to different profiles of tiles, connections between tiles and directions of tiles.
4. Demonstrational artifacts with various double-curvature profiles and surface textures to enrich the design space of Geodesy.

RELATED WORK

4D Printing and Self-folding

A group of HCI researchers have recently been working on a 4D printing technique to approximate 3D surfaces directly from 2D sheets to save transportation costs and printing time. 4D Printing [21] utilized programmable materials to transform shape memory lines into arbitrary 3D shapes. Recently, a great deal of work has been conducted with different material systems and computational methods that push forward 4D Printing. Transformative Appetite and BioLogic utilized hygromorphic transformations of food and natto cells to realize 2D to 3D shape changing [24, 25].

There are also closely relevant prior work which utilize the shape memory mechanism of thermoplastic to achieve self-folding mechanisms, including Thermorph [1] and 4DMesh [23]. While Geodesy is utilizing the same shrinkage property of thermoplastic as Thermorph and 4DMesh, the transformed shapes from three objects are different. Thermorph approximates shapes by re-meshing them into origami shapes with seams, 4DMesh processes them into a network of thin beams with holes in between, whereas all the textures produced by Geodesy are continuous surfaces without seams nor holes. Smooth hemisphere for instance, can only be processed by Geodesy. Using Thermorph, the result would be an origami hemisphere with around 20 flat polygonal faces and a “geodesic dome” with holes with 4DMesh. These geometries are also mechanically different. The seams and holes are all structural weak points. Lastly, comparing to 4DMesh, Geodesy methods are developed for much thinner objects, thus make morphing surface textures possible.

There is also a variety of research on micromaterial mechanisms for modeling the morphology of shape-changing sheets. The growth of leaves and tissues,

for example, is well studied [6, 12]. Shape-morphing plants can even be artificially created through Biomimetic 4D printing [8]. In comparison, Geodesy models the shape changing mechanism and uses an FDM 3D printer for fabrication.

Efficient Digital Manufacturing Strategy

A majority of programmable machines are invented for customizable manufacturing, like a 3D printer, knitting machine or laser cutter. However, some of these machines require a longer time to manufacture objects, and some come with limitations in their manufacturing properties. Today, researchers are inventing novel manufacturing techniques to either increase manufacturing efficiency or to push the boundaries of manufactured material properties. Examples of these are WirePrint [7]; a software system that assists users to print 3D wire structures [14]; LaserOrigami which utilizes laser cutting and gravity to produce 3D objects [15]; 3D Printed Hair which introduced a technique to print hair, fibers and bristles [11]; and Printing Teddy Bears which created a new printer to fabricate 3D objects from soft fibers [9]. Geodesy is novel in this context as it prints a single 2D sheet that can transform into 3D surfaces with deformable materials.

Inverse Design and Flattening/Mapping Algorithms

Many researchers are looking for geometric methods to fabricate non-active material units into 3D undevelopable surfaces, such as auxetic materials and tile decors [4, 10], inflatable structures [17, 20], and pre-stretched fabric tiles with constraints [18]. Compared to them, Geodesy uses an active shrinkable material to approximate similar target shapes without seams or joints.

In order to flatten a 2.5D surface into a 2D flat sheet, we have studied many computer graphics algorithms on texture mapping, such as Spectral Conformal mapping [16], Boundary First Flattening [19], Spin Transformation of Discrete Surfaces [5] and using developable surfaces to approximate double-curvature surfaces [3]. Unlike texture mapping which can arbitrarily transform and distort in a two dimensional world, Geodesy can only change the local area by directional shrinkage. Inspired by the many mapping algorithms stated above, we developed a purely geometric method for the inverse design methodology, and a tailored mass-spring model for simulation.

GEODESY METHOD

We leverage the known material mechanism- anisotropic shrinkage of thermoplastic from literature (including Thermorph [1] and 4DMesh [23]) for Geodesy. In Thermorph and 4D Mesh, the printing speed and bilayer ratio are used to control the shrinkage rate. However, in the case of Geodesy, which requires continuous printing and shrinkage tunability with a higher accuracy comparing with

the literature, another more suitable strategy for shrinkage ratio control is needed. Thus, we suggest a new printing strategy to tune the shrinkage rate: the layer thickness.

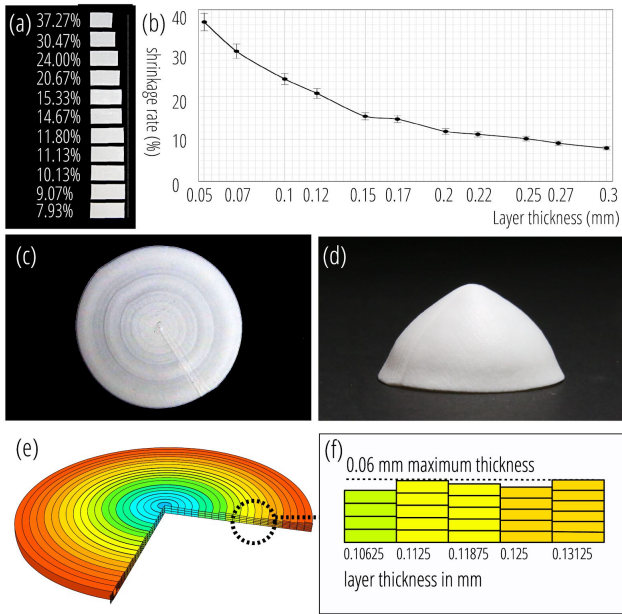


Figure 2. (a) Geodesy method. (b) Tests for the mapping between layer thickness and shrinkage rate. (c) Top view of a 2D flat sheet. (d) Side view of a single transformed texture. (e, f) Perspective diagram and cross section of the 2D sheet showing the change of the layer number.

Controlling different shrinkages of thermoplastic by modifying its layer height has been mentioned in one previous effort [13]. van Manen et al. provided a diagram in their supplementary with four data points that shows that lower layer height leads to higher built-in strain. This study though did not utilize this property for any its “shape-shifting” examples. We were inspired by this reported phenomenon, and leveraged this deformation mechanism and investigated it in a finer detail, with the intention of controlling local shrinkage rate by tuning layer thickness *on the fly in one continuous printing path*. We did 33 tests on rectangles with the same original length but different layer thicknesses to gain a thorough understanding of the phenomenon and in order to develop a precise control over the shrinkage rate. This knowledge allowed us to develop a design approach for printing full material sheets with variable shrinkage properties that leads to the formation of complex 3D objects.

As Fig. 2a shows, we can control the shrinkage ratio from 37.27% to 7.93% by changing the layer thickness with a standard printing speed at 3000 mm/min. We print sheets of material with a total thickness between 0.5mm and 0.6mm. Since the thickness of each printed layer ranges from

0.05mm to 0.3mm, multiple printing layers are needed to achieve the final total thickness of the sheet.

The whole thickness of the sheet is related to the stiffness and resistance to the curving of the sheet. To keep the stiffness of the sheet at a moderate level, we change the number of layers according to the layer thickness at each position. The number of layers printed for a particular layer thickness is $\text{trunc}(0.6/\text{layer-thickness})$. Since the sheet’s total thickness of 0.6mm cannot be divided by most values of available layer thickness options, there can exist discontinuous thickness changes that may lead to unpredictable local deformations and a reduction of strength.

Leveraging the property that thermoplastic only shrinks in printing direction, we introduce a path planning approach that gives the user a certain degree of controllability over the transformed 3D geometry of each tile (Fig. 2c, 2e). We extract the outline of the tile as the outermost path and shift it inward from the outline with same offset to produce a new closed path. Repeating this process until the new curve is too small to be shifted inward creates a series of closed paths with the same distance in between. Finally we connect the nested paths together to construct a single continuous path covering the whole 2D tile.

DESIGN COMPONENTS

Profile of a Single Tile

A profile is the outline of a single tile from a side view (Fig. 3). Through the manipulation of the shrinkage rate of each geodesic path, we can create textures with a variety of profiles that can self-transform from flat sheets. We can accurately inverse design the printing tool path of all the textures showed in the figure from given profiles, given that they are surfaces of revolution with axial symmetry. When outlines of textures go beyond circles, inverse design will not work exactly. However, if we apply the shrinkage distribution defined for circular textures to convex polygonal outlines, the transformed geometry would preserve the overall features and be visually similar to the corresponding geometry of circular tiles, such that both of the tiles have convex curvature or have a sharp summit.

Fig. 3 shows different profiles of a single tile. These profiles can be adapted for a group of connected tiles to form different surface textures as well (Fig. 16).

- Convex Texture: the shrinkage rate decreases from outer circles to inner circles (Fig. 3a).
- Concave Texture: the shrinkage rate increases from outer circles to inner circles (Fig. 3b).
- Texture with Curvature Transition: the shrinkage rate first decreases and then increases from outer circles to inner circles (Fig. 3c).

- Subtle Cone Texture: the shrinkage rate is uniform and small(11%) (Fig. 3d).
- Dramatic Cone Texture: the shrinkage rate is uniform and large(37%) (Fig. 3e).

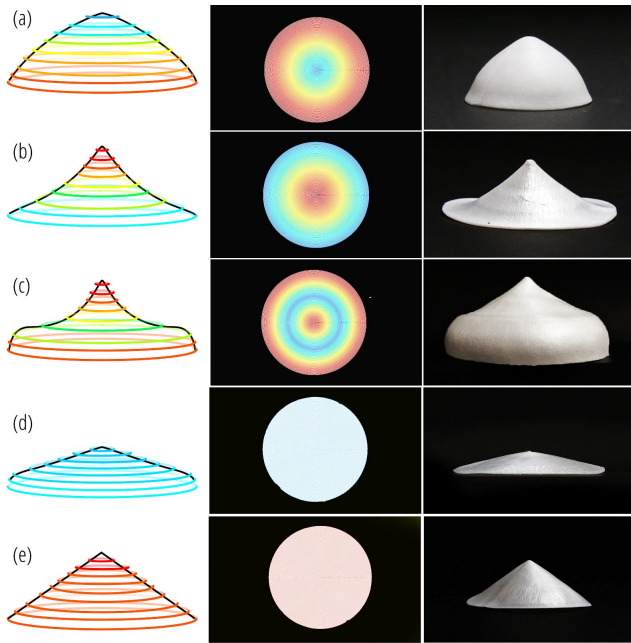


Figure 3. Different side profiles of Geodesy. Left column shows the target side view profile. Middle column shows the 2D printing tool path. Right column shows the transformed single texture.

Connection of Tiles

Beyond controlling the profile of each tile, we can create a surface with multiple textures by connecting tiles together through printing. The connection between tiles can be achieved by either printing two tiles directly attached to each other's edge or by printing a mesh structure in between tiles with plastic or elastic thermoplastic. For both cases, the relative rotation angles between two tiles are different and tunable.

After triggering two directly attached tiles, their center parts will rise respectively, which creates bending strain within the connection part. To release the bending strain, two tiles will rotate around the attachment axis, forming a rotation angle θ between the bottom surfaces of two textures. This produces a plastic 3D surface with local textures and an overall shape caused by the transformation of the textures (Fig. 4a and b). By introducing mesh connections between the tiles, the rotation angle can be decreased as the mesh can absorb a certain amount of bending strain, and form a smaller angle θ' (Fig. 4c and d).

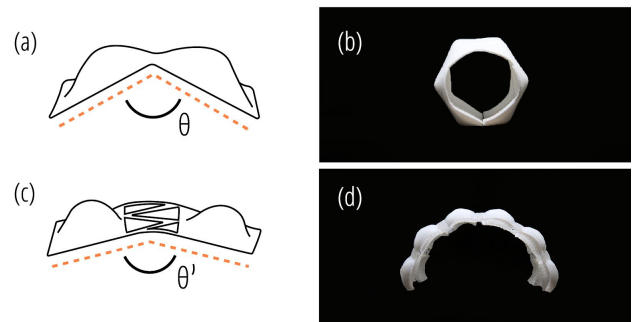


Figure 4. Bending curvature with different connection methods. (a) Tiles with direct connections in between. (b) Side view of a directly connect textured surface. (c) Tiles with flexible mesh connection in between. (d) Textured surface with flexible connection.

Flexibility of Tile Connections

If the neighboring two tiles are connected without a mesh (Fig. 4b), the structure is not very flexible. However, if the mesh connection is printed with soft plastic like TPU or PP, it will provide a certain flexibility for the morphed texture surface. Fig. 5a and b show the different deformation states of the same structure with flexible mesh connections.

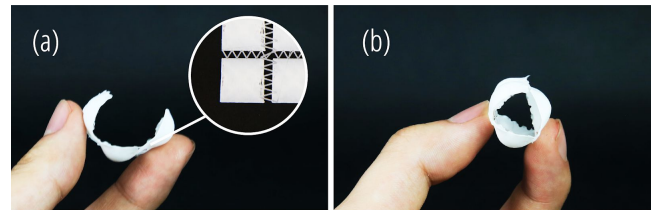


Figure 5. Flexibility of the mesh connection structure.

Directional Controllability of Tiles

The printed flat sheet has approximately uniform thickness from the bottom layer to the top layer. While the sheet is symmetric from both sides, the self-rising process is an asymmetric transformation, with each tile being able to rise both upwards and downwards. As a result, tiles will have a random rising direction causing an uncontrollable global geometry (Fig. 6c).

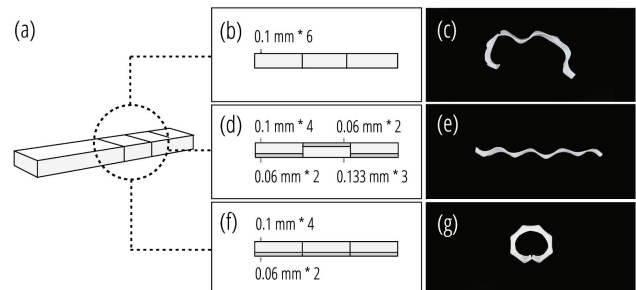


Figure 6. Directional controllability. (b, c) A randomly banding strip with uniform monolayer structure. (d, e) A flat strip by changing the thinner layer direction alternatively. (f, g) A ring-shaped strip with consistent thinner layer direction.

To control the rising direction, we developed a bilayer structure (Fig. 6d, 6f) that directs each tile to rise on the targeted side without excessively influencing the geometry of each texture.

FABRICATION PROCEDURE

Printing. Our project is focused on off-the-shelf FDM printing. In our fabrication procedure, we used a Makerbot Replicator 2X, with white Polymaker PLA as the printing material for tiles and plastic meshes, and transparent Polymaker PP for elastic meshes. While printing, we maintained a nozzle temperature of 200°C for PLA and 220°C for PP, with a standard printing speed of 3000 mm/min for tiles and 1500 mm/min for meshes.

Triggering. The sheet is placed in an environment that forces the material into its glass transition phase; ideally, this is in water heated to 87°C with minimal external elements present to influence the transformation. In our fabrications, we used a glass water tank of 11.9" x 7.1" x 7.1", or 2.6 gallons in volume. We used an Anova Culinary Immersion Circulator (800w) to heat and scale the liquid temperature.

Coloring. To place color designs on the forms, water-based ink was screen printed on flat, non-actuated Geodesy substrates. The screen mesh thread diameter and opening dimension between threads is 48 microns and 79 microns, respectively. The inks need to be fully air cured before activation, so it does not peel off the thermoplastic when actuated in hot water.

USER WORKFLOW

An interactive simulation-based platform is implemented to assist users with design, simulation and fabrication of Geodesy sheets.

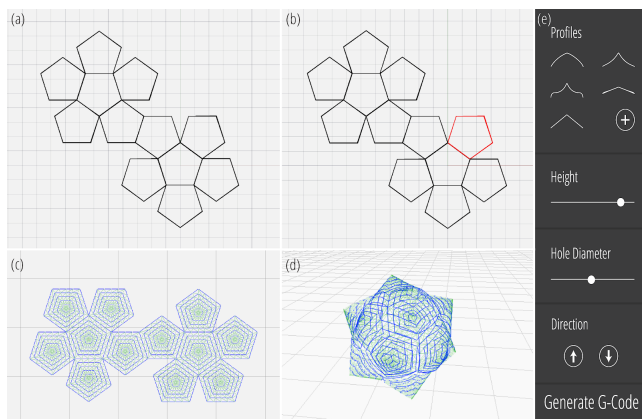


Figure 7. User workflow. (a). Users input outlines for tiles, (b). select one tile, (c) choose a profile from profile library, adjust the texture height, hole size and rising direction, (d) get the flat pattern and see the transformed geometry from simulator.

Design Profile for an Individual Tile

Users input a targeted profile of a tile (Fig. 3 left column). The software inversely designs the 2D printing pattern (Fig. 3 middle column), and outputs the shrinkage feature that defines how the shrinkage changes from the outer circles to the inner circles. The feature is then added to a profile library for the simulator (Fig. 7e).

Design Surface with Textures

The user creates the 2D outlines of all the tiles of the surface with commercial CAD tools and outputs them in the DXF file format (Fig. 7a).

After selecting a tile, the user can choose a profile from the profile library (Fig. 7e) mentioned in the previous step, and adjusts the parameters of the texture, including its height, rising direction, and whether or not it has a hole.

Simulator

The simulator will compute and display an approximated 3D geometry based on the user's outline and configuration (Fig. 7d). Once simulated, the user can iteratively modify the 2D outline and tile configurations until producing the desired simulation result.

G-code Generator

Finally, the software will export the corresponding G-code for printing.

PIPELINE

Extract the Shrinkage Feature of Each Tile

A purely geometric calculation is sufficient to compute the shrinkage properties of the flat concentric rings that produce a surface of revolution via the morphing process (Fig. 8). Given the axi-symmetric form of a surface of revolution, the shrinkage amount is a constant value for each ring. That shrinkage ratio is simply the circumference of the circle in its final 3D location (C_f) divided by the circumference of the circle in its initial flat location (C_i). We then define the shrinkage percentage as $Sh(k) = 1 - C_f/C_i$, where k specifies the k 'th circle.

The circumference of a circle is $C = 2\pi R$, where R is the radius of the circle. Plugging this formula into the formula for $Sh(k)$, the k 'th shrinkage percentage becomes $1 - R_f/R_i$. A single, cross-sectional parameterized curve $F(u)$ defines the outline of the surface of revolution. R_i is equal to $w \times k$, where w is the width of the printed lines. R_f can be computed as $F(G(R_i))$, where $G()$ is a function that computes a u value for a point on the curve that is distance R_i along the curve. The G-code needed to print the circles can then be generated from the computed Sh_k values. Given the limited shrinkage ratio range, which is from 7% to 37%, any shrinkage percentage outside of this range is not printable.

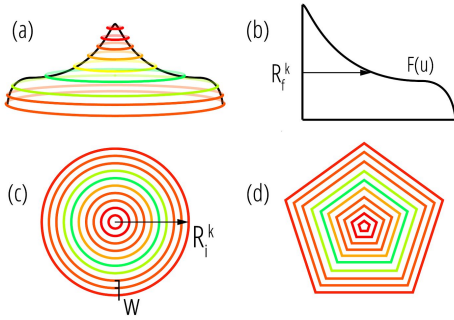


Figure 8. Map the shrinkage-radius relationship from a circle tile to a convex polygon tile.

In order to generalize the profile to textures with a convex polygonal outline, we map the shrinkage rate distribution from circular tiles to polygon tiles. To get the shrinkage rate of the j 'th path in the polygon tile, we define $Sh'(j) = Sh(\text{trunc}(j/N' * N))$, where N is the number of geodesic paths for the circular tile, and N' is the number of paths for a polygonal tile.

Simulator

Offset and Sampling

To initialize the simulation, the outlines of the textures should be converted into a structure that is compatible with the simulation model. For a given polygon outline of a tile, we shift all the edges inward by a constant offset, which is equal to the width of the printing path. This is repeated until the area surrounded by the outline is approximately zero, producing a series of nested outlines separated by a constant distance. We then evenly sample vertices along the outlines, calculate a correspondence between vertices in two neighboring outlines, and connect these vertices with edges according to their correspondences (Fig. 9).

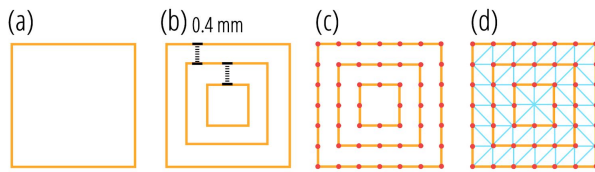


Figure 9. Offsetting and sampling

Mass Spring Model for Geodesy

We utilize the open source C++ library Shape-Up [2] to build a mass-spring model specifically for Geodesy (Fig. 10). We employ a projection-based solver to simulate the transformation of the printed pattern. First, the 2D pattern along with the printing loops are tessellated into triangles. Then we model the shrinkage of the material along the tangential direction of the printing curves as shrinkable springs imposed on the edges, such that the edge length $|p_{ij} - p_{i,j+1}|$ is constrained to shrink according to the shrinkage s_{ij} defined on it, while other edges between printing tool paths are static structural springs constrained to keep their length

unchanged; thus modeling the Young's modulus and the material mechanism of PLA only shrinking in the printing direction and not shrinking in the perpendicular direction. We also introduce bending springs to model the shear modulus of the material. Finally, we add instantaneous forces on a subset of the vertices to trigger the simulation, which models the directional control caused by the bilayer structure. We refer to Shape-Up [2] for the details of the solver. After the user is satisfied with the design, we generate toolpaths for 3D printing, as well as the printing layer thickness to control the shrinkage of the material on the toolpath.

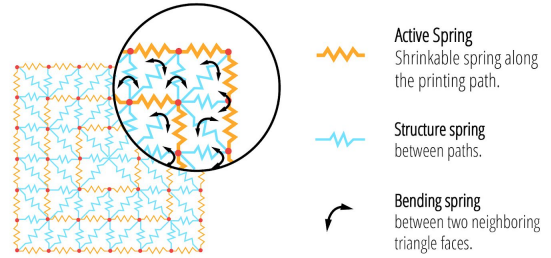


Figure 10. Spring Model diagram.

APPLICATIONS

As tiles are main morphing components, we try to demonstrate different design spaces by categorizing potential applications based on the numbers and sizes of these raised tiles on a surface.

A Single Tile

Spin tops are fascinating and poetic marriage between physics and play (Fig.11a-c). By adding a handle to two pairs of cones, we give them the simple function of being a toy. Each piece of the spin top is a large single texture that is separately printed and then quickly assembled post-actuation.

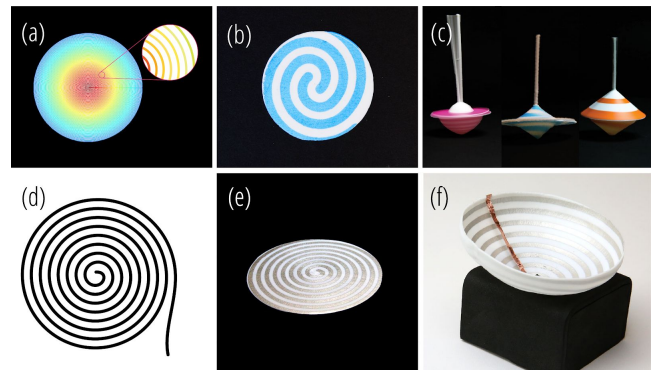


Figure 11. A single tile. (a) Visualization of the printing path and shrinkage rate of half of the spin top. (b) Printed flat spin top. (c) Assembled and functional spin tops. (d) Stencil for screen printing speaker coil. (e) Printed flat speaker with

conductive screen-printed ink. (f) Assembled cone speaker on a magnet.

A Network of Tiles

Polyhedron-based Self-folding Structures

Geodesy provides a unique approach to self-fold polyhedron structures from flat sheets. Unlike the conventional self-folding polyhedron that is similar to paper origami [1], Geodesy can produce double curvatures on each face of the polyhedron structure (Fig. 12a-b). We designed a helmet with a scaling factor of 6 (Fig. 12c-d).

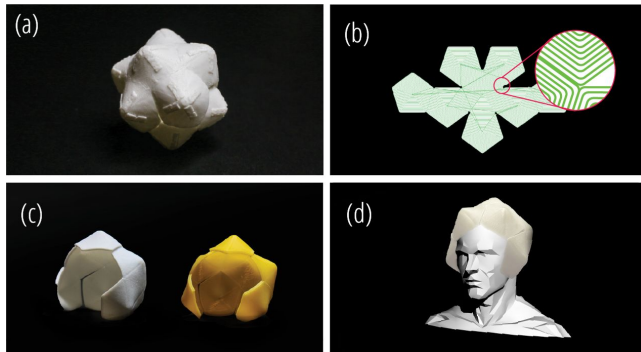


Figure 12. Polyhedron-based self-folding structures. (a) Polyhedron ball. (b) Printing path of helmets. (c, d) Helmets.

Groups of Large Raised Tiles

With Geodesy approach, one can control both the number and size of textures. Under the context of Geodesy, we define that if the tile numbers are within 10, with tile longest diameter longer than 3cm, the tiles are more perceived as individual features, thus we call them groups of large raised tiles.

In Fig. 13, mountainous landscape is designed to show a group of raised hills. In between each mountain is a printed rigid mesh.

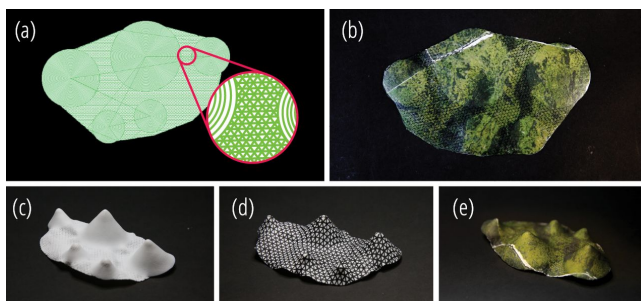


Figure 13. Mountainous landscape.

In Fig. 14, we aimed to create a model resembling an existing biogenetic texture. Here we take turtle shell as an example, with textures imitating each hump on turtle shell.

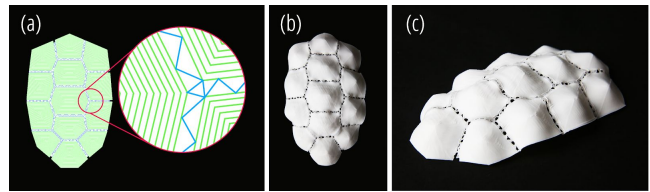


Figure 14. Turtle shell.

Groups of Small Raised Tiles - Surface Textures

In contrary to large raised tiles, if tile numbers are more than 10 and each tile diameter is smaller than 2mm, we call them groups of small raised tiles (i.e., surface textures).

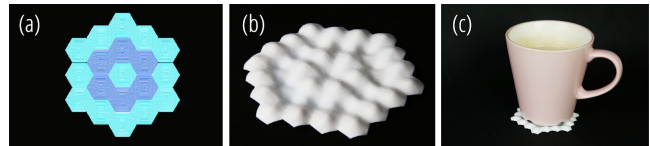


Figure 15. Textured coaster.

In Fig. 15, by controlling the rising direction of each tile, we keep the global shape of the sheet flat but generate textures on the surface as a coaster that helps to dissipate heat.

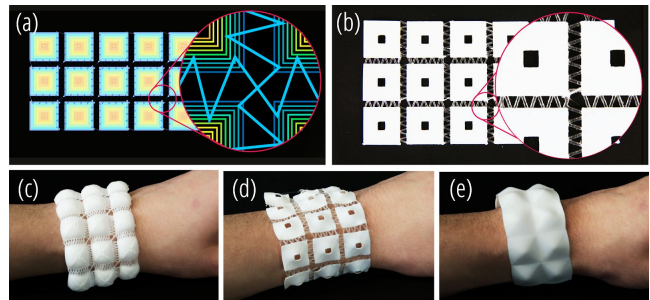


Figure 16. Bracelets with different textures.

In Fig. 16, by integrating the technique of profile control and soft mesh connections to increase flexibility of the morphed textures, we created conformable bracelets with different aesthetic qualities.

DISCUSSION AND LIMITATION

The bilayer structure used to control rising direction can sometimes introduce shape distortion that cannot be simulated. The structure can cause bending on the edge of tiles due to the different shrinkage rates of two layers. Comparatively in simulation, we model the directional control in a simplified way: by adding a triggering force pointing out to the desired direction of the plane. Due to this simplification, we cannot model some shape distortions caused by the bilayer.

The tile sizes are limited. If the tile sizes are too small, the thickness of the sheet cannot be ignored and will resist the shape change. However, the spring model in the simulation simplifies the Geodesy sheet as a monolayer. This simplified model cannot predict the behavior of small tiles.

In order to keep the tiles simulatable, tile sizes must be above a certain area.

The inverse design can only precisely determine the 2D configurations for axial symmetric shapes. When the outline of the texture is a convex polygon that has similar edge lengths but in a different direction, the geometry would share a very similar profile as the axi-symmetric one. But when the polygon becomes longer and narrower, the difference between the inputted inverse designed shape and the actuated shape would be much greater. Although the transformation of long and narrow tiles can still be simulated by the simulator with small errors, inverse design will no longer be able to instruct the user about the profile.

CONCLUSION

In this paper, we introduced a novel path planning approach for surfaces with self-rising continuous double-curvature textures. Through this work, we hope to empower designers to quickly customize and prototype such morphing surfaces, as well as enrich the toolbox of 4D printing and shape changing materials. We believe such accumulated advancements following the trajectory of 4D printing literature will enlarge the design space, the practicality, and applicability of FDM-based 4D printing. With the increasing design parameters from single-curvature to double-curvature surfaces; from smooth to textured surfaces; from rigid to flexible structures, we hope a growing community of designers and makers will join us in the journey of democratizing 4D printing.

REFERENCES

- [1] An, B., Tao, Y., Gu, J., Cheng, T., Chen, X. 'anthony', Zhang, X., Zhao, W., Do, Y., Takahashi, S., Wu, H.-Y., Zhang, T. and Yao, L. 2018. Thermorph: Democratizing 4D Printing of Self-Folding Materials and Interfaces. *Proceedings of the 2018 CHI Conference on Human Factors in Computing Systems* (New York, NY, USA, 2018), 260:1–260:12.
- [2] Bouaziz, S., Deuss, M., Schwartzburg, Y., Weise, T. and Pauly, M. 2012. Shape-Up: Shaping Discrete Geometry with Projections. *Computer graphics forum: journal of the European Association for Computer Graphics*. 31, 5 (Aug. 2012), 1657–1667.
- [3] Chen, H.-Y., Lee, I.-K., Leopoldseder, S., Pottmann, H., Randrup, T. and Wallner, J. 1999. On Surface Approximation Using Developable Surfaces. *Graphical Models and Image Processing*. 61, 2 (Mar. 1999), 110–124.
- [4] Chen, W., Ma, Y., Lefebvre, S., Xin, S., Martínez, J. and Wang, W. 2017. Fabricable Tile Decors. *ACM transactions on graphics*. 36, 6 (Nov. 2017), 175:1–175:15.
- [5] Crane, K., Pinkall, U. and Schröder, P. 2011. Spin Transformations of Discrete Surfaces. *ACM transactions on graphics*. 30, 4 (Jul. 2011), 104:1–104:10.
- [6] Dervaux, J. and Ben Amar, M. 2008. Morphogenesis of growing soft tissues. *Physical review letters*. 101, 6 (Aug. 2008), 068101.
- [7] Ding, Z., Weeger, O., Qi, H.J. and Dunn, M.L. 2018. 4D rods: 3D structures via programmable 1D composite rods. *Materials & design*. 137, (Jan. 2018), 256–265.
- [8] Gladman, A.S., Matsumoto, E.A., Nuzzo, R.G., Mahadevan, L. and Lewis, J.A. 2016. Biomimetic 4D printing. *Nature materials*. 15, 4 (Apr. 2016), 413–418.
- [9] Hudson, S.E. 2014. Printing Teddy Bears: A Technique for 3D Printing of Soft Interactive Objects. *Proceedings of the SIGCHI Conference on Human Factors in Computing Systems* (New York, NY, USA, 2014), 459–468.
- [10] Konaković, M., Crane, K., Deng, B., Bouaziz, S., Piker, D. and Pauly, M. 2016. Beyond Developable: Computational Design and Fabrication with Auxetic Materials. *ACM transactions on graphics*. 35, 4 (Jul. 2016), 89:1–89:11.
- [11] Laput, G., Chen, X. 'anthony' and Harrison, C. 2015. 3D Printed Hair: Fused Deposition Modeling of Soft Strands, Fibers, and Bristles. *Proceedings of the 28th Annual ACM Symposium on User Interface Software & Technology* (New York, NY, USA, 2015), 593–597.
- [12] Liang, H. and Mahadevan, L. 2009. The shape of a long leaf. *Proceedings of the National Academy of Sciences of the United States of America*. 106, 52 (Dec. 2009), 22049–22054.
- [13] van Manen, T., Janbaz, S. and Zadpoor, A.A. 2017. Programming 2D/3D shape-shifting with hobbyist 3D printers. *Materials horizons*. 4, 6 (Nov. 2017), 1064–1069.
- [14] Meinel, C., Plattner, H., Döllner, J., Weske, M., Polze, A., Hirschfeld, R., Naumann, F., Giese, H., Baudisch, P., Friedrich, T. and Müller, E. 2018. *Proceedings of the 10th Ph.D. Retreat of the HPI Research School on Service-oriented Systems Engineering*. Universitätsverlag Potsdam.
- [15] Mueller, S., Kruck, B. and Baudisch, P. 2013. LaserOrigami: Laser-cutting 3D Objects. *Proceedings of the SIGCHI Conference on Human Factors in Computing Systems* (New York, NY, USA, 2013), 2585–2592.
- [16] Mullen, P., Tong, Y., Alliez, P. and Desbrun, M. 2008. Spectral conformal parameterization. *Computer Graphics Forum* (2008), 1487–1494.
- [17] Ou, J., Skouras, M., Vlavianos, N., Heibeck, F., Cheng, C.-Y., Peters, J. and Ishii, H. 2016. aeroMorph

- Heat-sealing Inflatable Shape-change Materials for Interaction Design. *Proceedings of the 29th Annual Symposium on User Interface Software and Technology* (Oct. 2016), 121–132.

- [18] Pérez, J., Otaduy, M.A. and Thomaszewski, B. 2017. Computational Design and Automated Fabrication of Kirchhoff-plateau Surfaces. *ACM transactions on graphics*. 36, 4 (Jul. 2017), 62:1–62:12.
- [19] Sawhney, R. and Crane, K. 2017. Boundary First Flattening. *ACM transactions on graphics*. 37, 1 (Dec. 2017), 5:1–5:14.
- [20] Skouras, M., Thomaszewski, B., Kaufmann, P., Garg, A., Bickel, B., Grinspun, E. and Gross, M. 2014. Designing Inflatable Structures. *ACM transactions on graphics*. 33, 4 (Jul. 2014), 63:1–63:10.
- [21] Tibbits, S. 2014. 4D printing: multi-material shape change. *Architectural Design*. 84, 1 (2014), 116–121.
- [22] Tibbits, S., McKnelly, C., Olguin, C., Dikovsky, D. and Hirsch, S. 2014. 4D Printing and Universal Transformation. (2014).
- [23] Wang, G., Yang, H., Yan, Z., Ulu, N.G., Tao, Y., Gu, J., Kara, B. and Yao, L. 2018. 4DMesh: 4D Printing Self-Folding Non-Developable Mesh Surfaces. *Proceeding of the 2018 ACM Symposium on User Interface Software and Technology (UIST'18)* (2018), In Press.
- [24] Wang, W., Yao, L., Zhang, T., Cheng, C.-Y., Levine, D. and Ishii, H. 2017. Transformative Appetite: Shape-Changing Food Transforms from 2D to 3D by Water Interaction Through Cooking. *Proceedings of the 2017 CHI Conference on Human Factors in Computing Systems* (New York, NY, USA, 2017), 6123–6132.
- [25] Yao, L., Ou, J., Cheng, C.-Y., Steiner, H., Wang, W., Wang, G. and Ishii, H. 2015. bioLogic: Natto Cells as Nanoactuators for Shape Changing Interfaces. *Proceedings of the 33rd Annual ACM Conference on Human Factors in Computing Systems* (Apr. 2015), 1–10.